Life Sciences 222 (2019) 148–157

Contents lists available at ScienceDirect

Life Sciences

journal homepage: www.elsevier.com/locate/lifescie

TGN-020 alleviates edema and inhibits astrocyte activation and glial scar formation after spinal cord compression injury in rats

Jian Li[a], Zhiqiang Jia[b], Wen Xu[c], Weidong Guo[a], Mingchao Zhang[a], Jing Bi[d], Yang Cao[a], Zhongkai Fan[a,*], Gang Li[e,*]

[a] Department of Orthopedics, The First Affiliated Hospital, Jinzhou Medical University, Jinzhou 121000, China
[b] Department of Spinal Surgery, The Second Affiliated Hospital, Henan University of Science and Technology, Luoyang 471003, China
[c] School of Nursing, Jinzhou Medical University, Jinzhou 121000, China
[d] Department of Neurobiology, Key Laboratory of Neurodegenerative Diseases of Liaoning Province, Jinzhou Medical University, Jinzhou 121000, China
[e] Department of Orthopedics, Shanghai Tenth People's Hospital, Tongji University School of Medicine, Shanghai 200072, China

ARTICLE INFO

Keywords:
Edema
Glial scar
Spinal cord injury
TGN-020
Aquaporin 4

ABSTRACT

Aims: Identifying drugs that inhibit edema and glial scar formation and increase neuronal survival is crucial to improving outcomes after spinal cord injury (SCI). Here, we used 2-(nicotinamide)-1,3,4-thiadiazole (TGN-020), a potent selective inhibitor of aquaporin 4 (AQP4), to investigate the effects of TGN-020 on SCI in Sprague-Dawley rats.

Main methods: We compressed the spinal cord at T10 using a sterile impounder (35 g, 5 min), to induce moderate injury. TGN-020 (100 mg/kg) or an equal volume of 10% dimethyl sulfoxide was then administered via intraperitoneal injection. Neurological function was evaluated using the Basso-Beattie-Bresnahan open-field locomotor scale 1, 3, 7, 14, 21, and 28 days after SCI. The degree of edema was assessed via determination of the precise spinal cord water content 3 days after SCI. Expression levels of AQP4, glial fibrillary acidic protein (GFAP), proliferating cell nuclear antigen (PCNA), and growth-associated protein-43 (GAP-43) were determined via western blotting and immunofluorescence staining 3 days after SCI and 4 weeks after SCI. Numbers of surviving neurons and glial scar sizes were determined using Nissl and hematoxylin-eosin staining, respectively.

Key findings: Our results showed that TGN-020 promoted functional recovery at days 3, 7, 14, 21, and 28, as well as reduced the degree of edema and inhibited the expression of AQP4, GFAP, PCNA at days 3 after SCI. Furthermore, observations 4 weeks after SCI revealed that TGN-020 inhibited the glial scar formation and up-regulated GAP-43 expression.

Significance: TGN-020 can alleviate spinal cord edema, inhibit glial scar formation, and promote axonal regeneration, conferring beneficial effects on recovery in rats.

1. Introduction

Spinal cord injury (SCI) usually leads to permanent functional impairment and imposes a heavy burden on families and society [1]. Effective methods and strategies to promote functional neurological recovery after SCI are becoming increasingly important. SCI mainly involves two pathophysiological stages, primary and secondary. Unlike primary damage, secondary injury is reversible, and involves a series of pathological events including edema, glial scar formation, ischemia, electrolyte imbalance, excitotoxicity, apoptosis, and inflammation [2,3].

In cases where spinal cord edema occurs after SCI it generally occurs immediately thereafter, exacerbates secondary damage in neuronal tissues, and has substantial effects on subsequent neurological recovery [4]. Reducing edema has been shown to improve recovery from SCI [5,6]. Aquaporin 4 (AQP4) is a major water-selective channel protein of the aquaporin family that is found in laminae I and II at the boundaries of the ventral horns, and in the regions around the central canal and glia limitans, expressed predominantly in astroglial foot processes

Abbreviations: AQP4, aquaporin 4; BBB scores, Basso-Beattie-Bresnahan scores; CNS, central nervous system; DAPI, 4′, 6-diamidino-2-phenylindole; GAP-43, growth-associated protein-43; GFAP, glial fibrillary acidic protein; PCNA, proliferating cell nuclear antigen; SCI, spinal cord injury; TGN-020, 2-(nicotinamide)-1,3,4-thiadiazole

* Correspondence to: Z.K. Fan, Department of Orthopedics, The First Affiliated Hospital of Jinzhou Medical University, JinZhou 121000, China; G. Li, Department of Orthopedics, Shanghai Tenth People's Hospital of Tongji University, Shanghai City 200072, China.
E-mail addresses: fanzk_ln@163.com (Z.K. Fan), ganglili@126.com (G. Li).

https://doi.org/10.1016/j.lfs.2019.03.007
Received 9 December 2018; Received in revised form 21 February 2019; Accepted 5 March 2019
Available online 06 March 2019

surrounding neurons and blood vessels [7]. It is directly involved in the formation [8,9] and elimination [10,11] of edema, both of which differ depending on edema type [12]. In numerous previous studies, AQP4 deletion or downregulation reduced the degree of edema and improved neurological outcomes in models of cytotoxic edema induced by ischemic injury in brain and spinal cord [8,9,13].

The roles of SCI-induced reactive astrogliosis around the injured regions change over time [14,15]. Initially, astrocytes release various neurotrophins and restrict the pervasion of inflammation, thus promoting axonal regeneration after SCI [16,17]. Later, reactive astrocytes become hypertrophic and proliferative, and migrate toward the injured site where they eventually form a dense network of glial scarring that acts as a physical and chemical barrier and prevents repair and regeneration of damaged neural tissues [18,19]. It has been reported that in murine models of various types of brain injuries, AQP4 is also involved in processes that are unrelated to edema, including astrocyte migration and glial scar formation [20–22]. Previous studies in AQP4-deficient mice have shown that astroglial proliferation was inhibited in a 1-methyl-4-phenyl-1,2,3,6-tetrahydropyridine-induced Parkinson's disease model [23]. These findings suggest that modulation of AQP4 expression or function may influence reactive astrogliosis in some CNS diseases.

It has been reported that 2-(nicotinamide)-1,3,4-thiadiazole (TGN-020) selectively inhibits AQP4 [24–26]. TGN-020 can evidently significantly reduce glutamate-induced increases in AQP4 and glial fibrillary acidic protein (GFAP) expression in vitro [27], block the influx of subarachnoid cerebrospinal fluid into the spinal parenchyma [28], and increase regional cerebral blood flow in normal mice [29]. A single dose of TGN-020 can also reportedly inhibit focal ischemic reperfusion-induced brain edema, reduce infarct volumes [25,30,31] and prevent methamphetamine-induced brain edema, blood-brain barrier disruption, and behavioral impairment via the downregulation of AQP4 expression [32]. To date, few studies have investigated the effects of TGN-020 on SCI in rats. In the current study, we investigated the effects of TGN-020 on edema, astrocyte proliferation, and glial scar formation in vivo after moderate spinal cord compression injury in a rat model, to assess its potential as a new pharmacological agent for the treatment of secondary injury after SCI.

2. Materials and methods

2.1. Animals and experimental groups

A total of 150 adult female Sprague-Dawley rats (180–220 g, 9–10 weeks old) were purchased from the animal center of Jinzhou Medical University (Jinzhou, China) and maintained under standard temperature conditions (23 ± 0.5 °C) with a 12 h light/dark cycle, food and water ad libitum were provided. All animal experiments were carried out in accordance with the Institutional Animal Care and Use Committee of guidelines of the Jinzhou Medical University. Great effort was made to reduce animal suffering. Animals were then randomly assigned to the following three groups: Sham group (n = 35) which were only subject to laminectomy without compression of spinal cord, SCI group (n = 35) which underwent 35 g impounder compression for 5 min at T10, TGN-020 group (n = 35) which received TGN-020 (Sigma-Aldrich, 100 mg/kg, i.p.) immediately followed SCI. Each group was equally and randomly assigned into four subgroups (n = 5 or 6 and 8/group) for the following experiments: (A) Spinal cord water content determination; (B) Western blotting; (C) Immunofluorescent assay, Hematoxylin-Eosin staining and Nissl staining; and (D) Locomotor function test. These rats in all groups were sacrificed 3 day or 4 weeks after injury.

2.2. Surgical procedures and TGN-020 administration

Basic surgical procedures and compression injury were performed as described previously [33]. All surgeries were performed under sterile conditions. Briefly, the rats were anesthetized with 10% chloral hydrate (0.33 mL/kg, i.p.). Once anesthesia took effect, surgical area was clean shaved and sterilized with 75% ethanol, a 3 cm dorsal longitudinal incision was made over the midthoracic spinal cord at T9–T12 and then removed peripheral paraspinal soft tissues to expose the spinal cord, leaving the dura intact. The spinal cord was extradurally compressed with a metal impounder (35 g, 5 min) gently loaded onto T10 level of the spinal cord to achieve a moderate injury (Fig. 1). Following surgery wounds were then closed in layers using 4–0 silk. Postoperativaly, TGN-020 (100 mg/kg, i.p.) diluted in 10% dimethyl sulfoxide (DMSO, Sigma-Aldrich) was administrated to TGN-020 group [30,31]. The concentration of DMSO was adjusted at 0.1% before injection. The Sham group and SCI group received the equal volume DMSO intraperitoneally at the same time. The animals were returned to individual cages once them were waked. During the postoperative recovery period, ceftriaxone sodium (50 mg/kg, i.p.) was administered on three consecutive days. The bladders were manually pressed three times daily until natural voiding reflex recovery, food and water were available ad libitum. Animals that behaved any abnormal neurological signs would be excluded from experiments.

2.3. Spinal cord water content determination

Spinal cord water content was measured using wet-dry weighting method to calculate the edema as previously described [34,35]. Briefly,

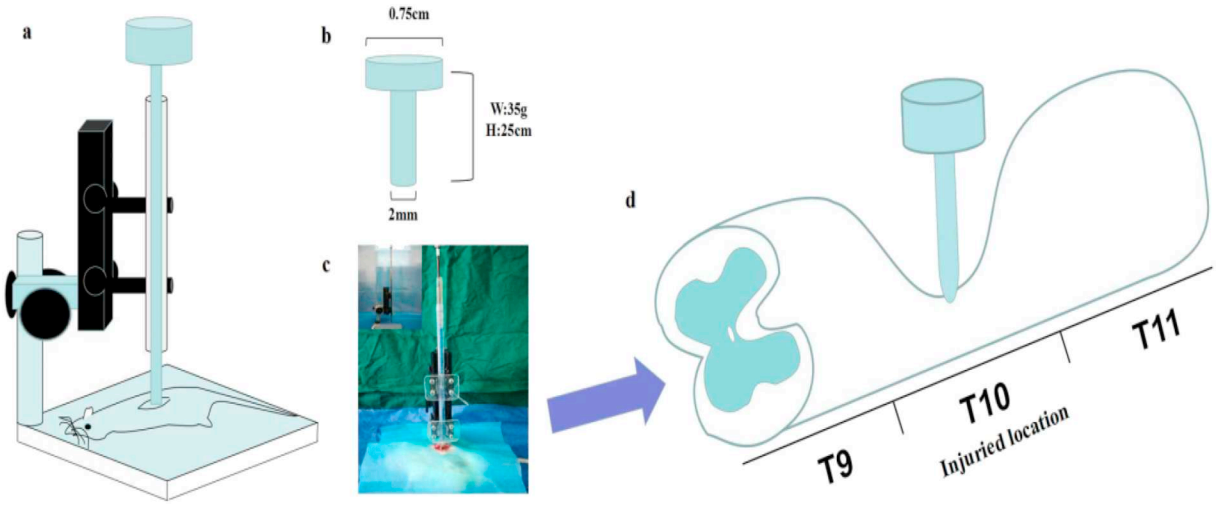

Fig. 1. Experimental paradigm: schematic of the spinal cord compression injury (a, b, c, d), which was established by a sterile impounder (35 g) to compress T10 spinal cord for 5 min and then removed immediately in rats.

animals were deeply anesthetized with 10% chloral hydrate 3 days after surgery in each group. The spinal cord was exposed layer by layer through the original surgical incision. A 1 cm spinal cord along the injury epicenter was removed immediately before being placed on a highly sensitive analytical balance (METFLERAE 26) for weighing (wet weight). Subsequently, the spinal cord were dried at 80 °C baking box for 48 h until a constant weight (dry weight), percentage water content of spinal cord was calculated as the formula: (wet weight − dry weight) / wet weight × 100%.

2.4. Western blotting analysis

Spinal cords (1 cm) centered on the injury site were removed at 3 days or 4 weeks and washed gently with deionized water to clear the impurity. Tissue lysates were centrifuged (12,000 rpm, 25 min) in a microcentrifuge at 4 °C after being lysed and homogenized in RIPA buffer (30 min) containing phenylmethane sulfonyl fluoride (PMSF) (Beyotime Biotechnology, Beijing, China) on frozen ice, protein quantities were determined using the BCA method in a spectrophotometer. Samples supernatants (40 μg/lane) was subjected to 10% sodium dodecyl sulfate-polyacrylamide gel electrophoresis (SDS-PAGE) and electrophoretically transferred onto a 0.45um polyvinylidene difluoride (PVDF) membranes (Millipore, Germany). Subsequently, the membranes were blocked with 5% non-fat milk diluted with TBST (25 mM Tris-HCl, 0.15 M saline, and 0.1% Tween-20) for 2 h at room temperature (RT). After being washed 3 times with TBST, the membranes were incubated with the following primary antibodies overnight at 4 °C: mouse anti-AQP4 (ab9512, 1:500), rabbit anti-GFAP (ab7260, 1:2000), mouse anti-PCNA (ab29, 1:2000), rabbit anti-GAP-43 (ab16053, 1:1000) (all from Abcam, USA), and β-actin (sc-47778, 1:400, Santa Cruz Biotechnology, USA). The day after, the membranes were incubated with the appropriate HRP-conjugated secondary goat anti-rabbit or anti-mouse IgG (7074P2/7074P6, 1:2000, Cell Signaling Technology, CST) respectively at RT for 2 h after being washed three times with TBST, the signals were visualized using enhanced chemiluminescent reagents (WKLS0l00, Millipore, USA). Image J software (Media Cybernetics, Georgia, MD, USA) was used to semi-quantify the protein level in every lane.

2.5. Sections preparation

At 3 days or 4 weeks after surgery, rats were deeply anesthetized with 10% chloral hydrate and perfused through the heart with ice-cold 0.9% saline followed by 4% paraformaldehyde (PFA) in 0.1 M phosphate-buffered saline (0.1% PBS, pH 7.4). The T9–T12 spinal cords were excised and postfixed in the perfusate at 4 °C for 1 day and then dehydrated with 30% sucrose in PBS over 2 nights. Upon arrival in our need, spinal cord (1 cm) was removed and embedded in O.C.T. compound (4583, SAKURA, USA) for cryosectioning. Either cross or longitudinal serial frozen sections were cut at 10 μm thick around the boundary zone of the injury for the Immunofluorescence staining or Hematoxylin-Eosin (HE) staining and Nissl staining study using a cryostat microtome (CM3050S, Leica, Heidelberg, Germany). All tissue sections were stored at −20 °C until they were conducted.

2.6. Immunofluorescent dual-labeling staining

Tissue sections were thawed and air-dried for 3–4 h in room temperature before being washing with 0.1%PBS. The sections were blocked with 5% normal goat serum (005-000-121, Jackson, USA) at 37 °C for 1 h to block the nonspecial sites and then was incubated with the following antibodies diluted in 5% normal goat serum: mouse anti-AQP4 (ab9512, 1:100), rabbit anti-GFAP (ab7260, 1:500) and mouse anti-PCNA (ab29, 1:200) (all from Abcam, USA) overnight in a humidified chamber at 4 °C. The following day, we washed sections with 0.1% PBS (3 × 5 min) prior to incubate with appropriate fluorescent secondary antibodies conjugated with Alexa Fluor 488 goat anti-rabbit IgG or Alexa Fluor 594 goat anti-mouse IgG (A-11034/A-11005, 1:250, Thermo Fisher Scientific) for 2 h at RT. Afterward, sections were rinsed with 0.1% PBS (3 × 5 min) and the nuclei were stained with 4′, 6-diamidino-2-phenylindole (DAPI) (D9542, 1:1000, Sigma-Aldrich, USA) diluted in deionized water for 6–8 min. All sections were observed by a fluorescence microscope (DMI4000B, Leica, Wetzlar, Germany). The optical density of fluorescence was analyzed using Image J software.

2.7. HE staining

HE staining was performed as described previously [36]. Briefly, longitudinal sections were stained sequentially with hematoxylin for 2 min and eosin for 15 s after washing in deionized water for 5 min, the sections were then dehydrated and mounted. A center section among the serial sections was used for data presentation. The stained images were used to measure the lesion volume using the Image J program (Media Cybernetics, Georgia, MD, USA).

2.8. Nissl staining

Transverse frozen sections were dried for about 2–3 h and soaked directly into a 1:1 solution of 100% ethanol and chloroform overnight in the dark. The following day, slides were then consecutively put in a solution of 100% ethanol and 95% ethanol for 1 min respectively. Afterward, put in deionized water for 1 min. Whereafter, slides were then transferred to a crystal violet solution (Beyotime Biotechnology, Beijing, China) whose temperature maintained in 37–50°Cfor 5 min to achieve optimal staining and washed quickly in deionized water. Subsequently, slides were dipped in 95% ethanol for 30 s and 100% ethanol and xylene soaked for 5 min twice respectively and mounted using neutral gum. The Nissl-positive cells were counted in four random chosen fields (× 200) at ventricornu on optical microscope (DMI4000B, Leica, Wetzlar, Germany). Five rats were examined per group. Quantification of normal motor neurons was analyzed with image-processing software (Media Cybernetics, Georgia, MD, USA).

2.9. Behavioral analysis

We evaluated locomotor function at 1, 3, 7, 14, 21, and 28 day post-surgery using the Basso-Beattie-and Bresnahan (BBB) open-field locomotor rating scale arranging from 0 to 21 rating scale [37]. Where 0 point denotes complete hind limb paralysis and 21 points denote normal locomotion function, these scores were conducted by at least three observers who were blind to the group assignment. Behavioral testing was first done at 24 h after injury and then weekly throughout the 28-day survival period in a noise-free environment.

2.10. Statistical analysis

All data were expressed as the mean ± SEM obtained from at least three independent experiments, Comparisons between two groups were analyzed by unpaired Student's *t*-test, more than two groups were performed with a one-way analysis of variance (ANOVA) with the least significant difference (LSD) post hoc test followed by using SPSS 17.0 for Windows (SPSS Inc., Chicago, IL, USA). A value of $p < 0.05$ was regarded as statistically significant.

3. Results

3.1. TGN-020 and spinal cord edema alleviation at day 3 after SCI

We measured the water content of tissue to reflect the level of edema at the site of SCI. At day 3 after SCI, a focal compression of the spinal cord at T10 in the SCI and TGN-020 groups resulted in visible

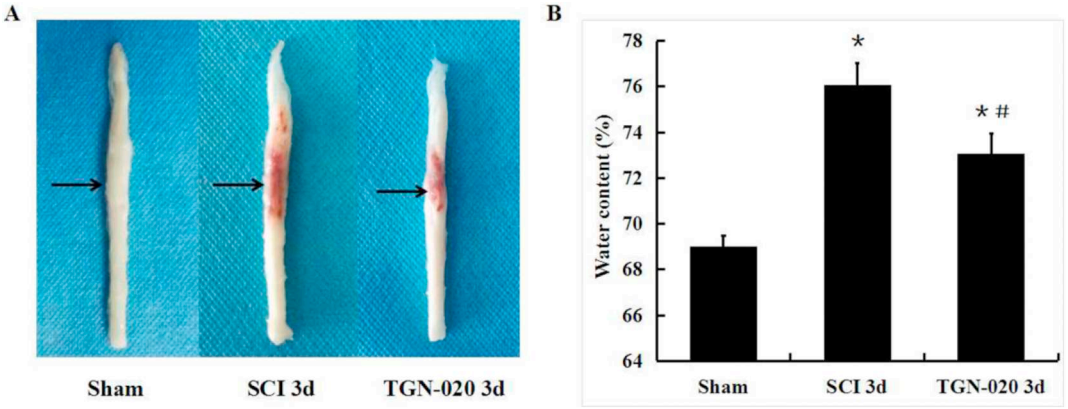

Fig. 2. Effects of TGN-020 on spinal cord edema at 3 days after SCI. (A) The gross photographs of the dissected spinal cord taken at 3 day after the rat SCI in each group. (B) Quantitative analysis of spinal cord water content. Data are expressed as mean ± SEM, $p < 0.05$ was considered significant ($n = 8$. $^{*}p < 0.01$ versus the sham group; $^{\#}p < 0.05$ versus the SCI group).

damage that was not evident in the sham group. Hemorrhaging and necrosis were obvious in the centers of injured spinal cords, and injured areas were substantially more affected in the SCI group than in the TGN-020 group (Fig. 2A). Photographs of injured spinal cords were reasonably consistent with calculations of spinal cord water content in each group (Fig. 2B). The water content of tissue in the segments adjacent to the injury site at day 3 was significantly higher in the SCI group (76.09 ± 0.93) and the TGN-020 group (73.07 ± 0.87) than it was in the sham group (69.02 ± 0.45) ($p < 0.01$). Spinal cord water content was significantly lower in the TGN-020 group (73.07 ± 0.87) than in the SCI group (76.09 ± 0.93) ($p < 0.05$), suggesting that TGN-020 could significantly reduce increased water content caused by SCI.

3.2. TGN-020 and reduced AQP4 expression at day 3 after SCI

Compared with the sham group, AQP4 expression was significantly increased in and around the centers of injured sites 3 days after compression injury in the SCI group ($p < 0.01$) and in the TGN-020 group ($p < 0.05$) (Fig. 3A, B). In the TGN-020 group, AQP4 expression was significantly lower than it was in the SCI group ($p < 0.05$). The results of immunofluorescence staining for AQP4 with GFAP were consistent with the results of western blotting (Fig. 3C, D). At day 3, AQP4 fluorescence intensity was significantly higher in both the SCI group and the TGN-020 group than it was in the sham group ($p < 0.01$), and it was significantly lower in the TGN-020 group than it was in the SCI group ($p < 0.05$). These data indicated that TGN-020 could down-regulate AQP4 expression, resulting in alleviation of spinal cord edema formation.

3.3. TGN-020 and inhibition of astrocyte proliferation at day 3 after SCI

GFAP, a cytoskeletal intermediate filament protein, is used as a specific astrocyte marker [38]. Proliferating cell nuclear antigen (PCNA) is a well-known marker of cell proliferation [39]. To investigate whether AQP4 is relevant to astrocyte proliferation in SCI, we examined PCNA and GFAP expression 3 days after SCI. Western blotting suggested that GFAP levels were low and virtually no PCNA was expressed in the sham group (Fig. 4A–C). Notably however, compared with the sham group there were significant increases in the expression of GFAP and PCNA around the centers of the injury sites at day 3 in the SCI group and the TGN-020 group ($p < 0.01$). At day 3, GFAP and PCNA expression were significantly lower in the TGN-020 group than they were in the SCI group ($p < 0.05$).

Double-staining to investigate coexpression of GFAP and PCNA in SCI yielded results that were consistent with the results of western blotting. As shown in Fig. 4D–F, GFAP-positive cells and PCNA-positive cells were scarce in the sham group. At day 3, compared with the sham group there were significantly more GFAP-positive cells and PCNA-positive cells around the injured area in both the SCI group and the TGN-020 group ($p < 0.01$). In the TGN-020 group, there were significantly less GFAP-positive cells and PCNA-positive cells than there were in the SCI group ($p < 0.05$). These results indicated that the AQP4 inhibitor TGN-020 could significantly inhibit the proliferation of astrocytes at day 3 after SCI.

3.4. TGN-020 and glial scar formation and axon regeneration at 4 weeks after SCI

To investigate whether TGN-020 administration could protect spinal cord tissues from being damaged at 4 weeks after SCI, we calculated the size of the cavity area to assess astroglial scar formation [36]. At 4 weeks, spinal cords were normal in the sham group but in both the SCI group and the TGN-020 group they exhibited destruction, including very large and irregular cavities (Fig. 5A, B). Cavity area was significantly smaller in the TGN-020 group than it was in the SCI group ($4.2 \pm 0.6\,mm^2$ vs. $3.0 \pm 0.4\,mm^2$, $p < 0.01$). These observations suggested that TGN-020 significantly reduced secondary spinal cord tissue degeneration after SCI.

To further explore the effects of TGN-020 on axonal regeneration, at 4 weeks after SCI we used western blotting to measure the expression of growth-associated protein-43 (GAP-43) (Fig. 5C, D), which is reportedly a marker of neurite growth in the CNS [40]. Compared with the sham group in which GAP-43 expression was relatively low, it was significantly upregulated in the SCI group at 4 weeks after SCI ($p < 0.01$), indicating regeneration of injured spinal cord. In the TGN-020 group, GAP-43 expression was greater than it was in the SCI group ($p < 0.05$). These results suggested that TGN-020 could reduce astroglial scar formation by reducing the size of the cavity, and promote axonal regeneration after SCI.

3.5. TGN-020 and neuron survival at 4 weeks after SCI

SCI-induced neuronal necrosis and apoptosis lead to neuronal loss. Nissl staining was performed on transverse sections at 4 weeks after SCI to investigate potential neuroprotective effects of TGN-020. Large numbers of Nissl-positive neurons with an extension cell body were

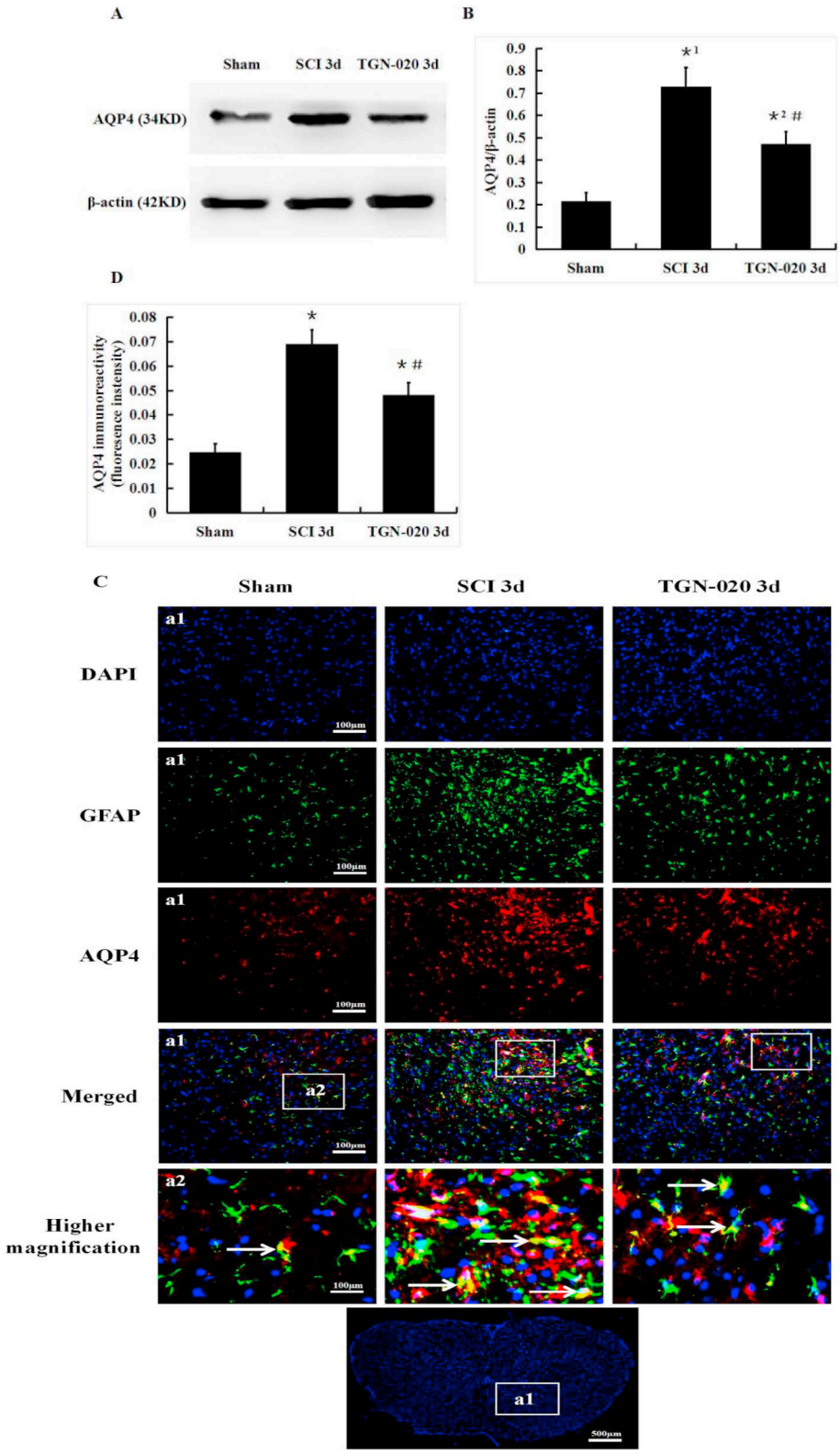

Fig. 3. Effects of TGN-020 on the expression of AQP4 at 3 days after SCI. (A–B) Western blotting and quantitative analysis of AQP4 ($n = 6$). Data are expressed as mean ± SEM, $p < 0.05$ was considered significant ($^{*1}p < 0.01$ versus the sham group; $^{*2}p < 0.05$ versus the sham group; $^{\#}p < 0.05$ versus the SCI group). (C–D) AQP4 (red)/GFAP (green)/DAPI (blue) triple labeling and quantitative analysis of AQP4 ($n = 5$). White arrows indicated co-localization of AQP4 with GFAP. Data are expressed as mean ± SEM, $p < 0.05$ was considered significant ($^{*}p < 0.01$ versus the sham group; $^{\#}p < 0.05$ versus the SCI group. Scale bars: 100 μm or 500 μm). (For interpretation of the references to color in this figure legend, the reader is referred to the web version of this article.)

detected, mainly in the ventral horns of normal spinal cords (Fig. 6B). Therefore, Motor neurons were detected at the anterior angle of injured spinal cords. As showed in Fig. 6A, In the sham group, the neurons exhibited an integrative and granular-like morphology, and large and numerous Nissl bodies indicating substantial protein synthesis in neural cells. In the SCI group, the neurons exhibited shrunken cell bodies, pyknotic nuclei, and irregular morphology, and intracellular toluidine blue staining was reduced around the lesions. In addition, the numbers of surviving motor neurons were significantly lower than they were in the sham group (Fig. 6C, $p < 0.01$). In the TGN-020 group, the numbers of surviving motor neurons were also significantly lower than they were in the sham group (Fig. 6C, $p < 0.01$), but neuronal morphology was better than it was in the SCI group, with deeper staining in the cytoplasm and significantly less loss of Nissl granules (Fig. 6C,

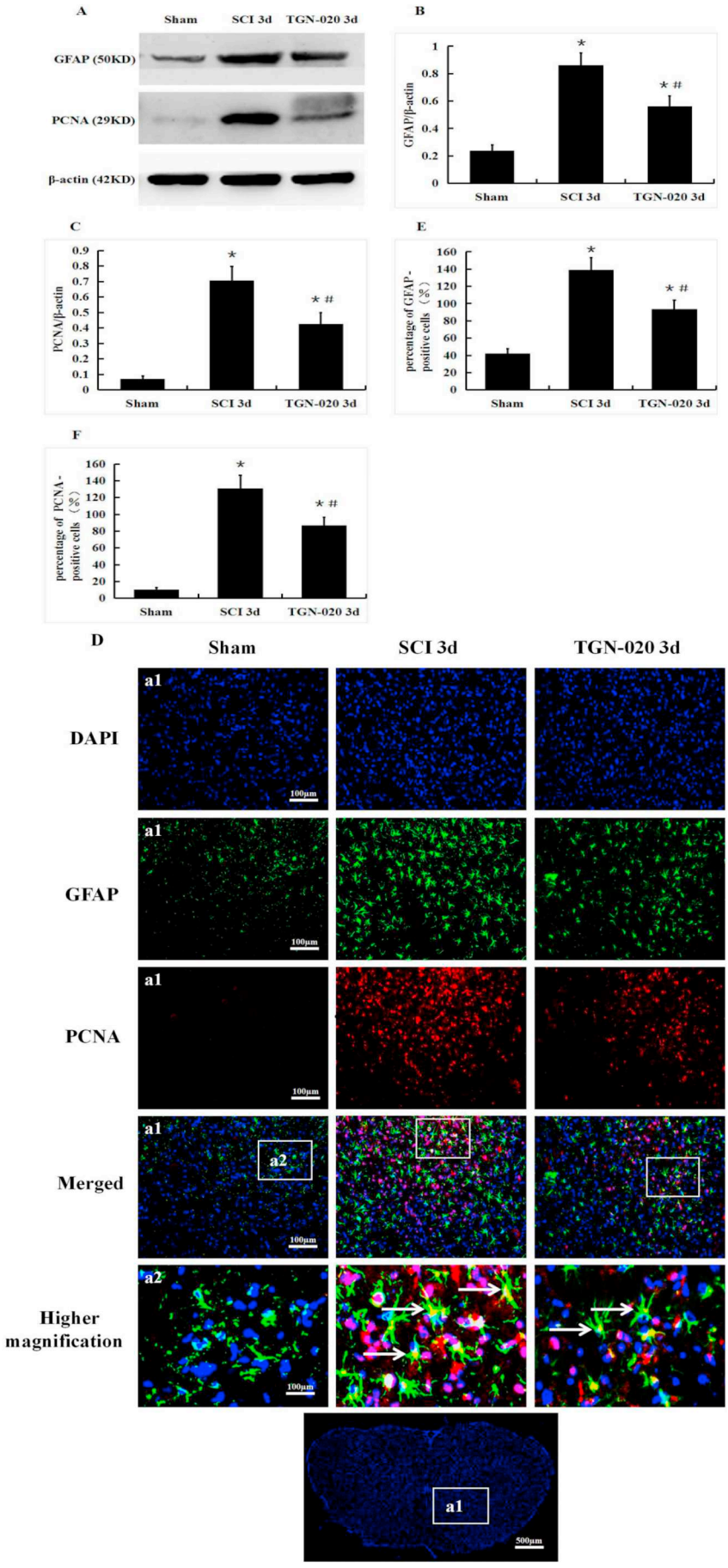

Fig. 4. Effects of TGN-020 on astrocyte proliferation at 3 days after SCI. (A–C) Western blotting and quantitative analysis of GFAP (A, B) and PCNA (A, C) ($n = 6$). (D–F) PCNA (red)/GFAP (green)/DAPI (blue) triple labeling and quantitative analysis of GFAP (D, E) and PCNA (D, F) ($n = 5$). The yellow color visualized in the merged images represented coexpression of PCNA/GFAP, white arrows indicated proliferative astrocytes. Data are expressed as mean ± SEM, $p < 0.05$ was considered significant ($^{*}p < 0.01$ versus the sham group; $^{\#}p < 0.05$ versus the SCI group. Scale bars: 100 μm or 500 μm). (For interpretation of the references to color in this figure legend, the reader is referred to the web version of this article.)

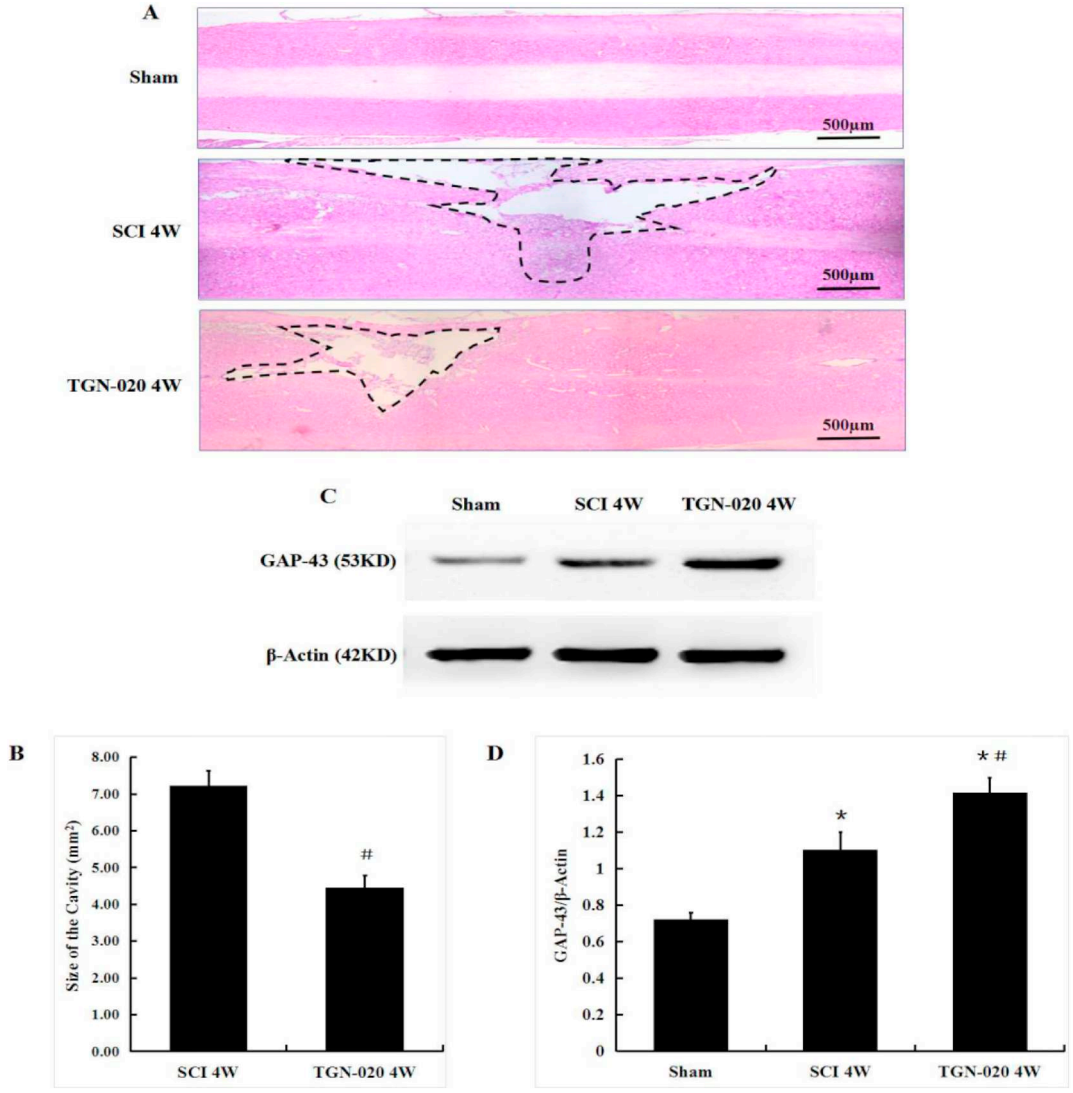

Fig. 5. Effects of TGN-020 on the glial scar formation and the expression of GAP-43 at 4 weeks after SCI. (A) Representative images of HE staining to measure cavity area. The dot lines in the images indicated the border of the cavity area. Sham group exhibited the normal morphorphy of longitudinal spinal cord, SCI showed an extensive lesion cavity and TGN-020 group shows reduced cavitation. Scale bars: 500 μm. (B) Quantitative analysis of lesion cavity area (mm^2) at 4 weeks in SCI group and TGN-020 group. Data are expressed as mean ± SEM, $p < 0.05$ was considered significant ($n = 5$, $^{\#}p < 0.01$ versus the SCI group). (C, D) Western blotting and quantitative analysis of GAP-43. Data are expressed as mean ± SEM, $p < 0.05$ was considered significant ($n = 5$, $^{*}p < 0.01$ versus the sham group; $^{\#}p < 0.05$ versus the SCI group).

$p < 0.01$). These results suggested that TGN-020 administration inhibited the loss of neurons.

3.6. TGN-020 and the promotion of functional locomotor recovery after SCI

To evaluate the effects of TGN-020 on functional locomotor recovery in rats after SCI, behavioral outcomes were assessed at days 1, 3, 7, 14, 21, and 28 via the Basso-Beattie-Bresnahan (BBB) scale, which has been widely used to evaluate the recovery of hindlimb motor function after SCI in rats. The sham group yielded a score of 21 at all time-points, reflecting normal motor function, whereas in the SCI group and the TGN-020 group BBB scores were reduced at 1 day after compression injury, then gradually increased to varying extents over time (Fig. 7). This indicated gradual recovery of locomotor function after SCI. In the TGN-020 group, BBB scores were significantly higher than they were in the SCI group at all time-points from day 3 to day 28 after SCI ($p < 0.01$ for day 7; $p < 0.05$ for days 3, 14, 12, and 28). These results suggest that TGN-020 administration can markedly promote the recovery of locomotor function in rats after SCI.

4. Discussion

Experimental compression of the spinal cord is clinically relevant to numerous human situations involving traumatic SCI, such as weight-drop, impactor transection, distraction, clip, forceps compression, and impounder compression [41]. In accordance with our experimental aims, in the current study we used a previously described modified compression device with a sterile impounder [33] instead of clip and forceps compression, to reduce the complexity of the subsequent surgery. TGN-020 at a dose of 5 mg/kg administered via intraperitoneal injection is known to exert anti-inflammatory [42] and anti-edema [27] effects in response to various central and peripheral nervous system injuries via the attenuation of AQP4 expression. In our preliminary study, 5 mg/kg TGN-020 administered intraperitoneally significantly reduced edema and astrocyte proliferation at day 3 after SCI. Notably however, that dosage was not associated with any substantial changes in histopathology results and neuroprotective effects on the axonal regeneration at 4 weeks, which may have been attributable to effects pertaining to TGN-020 metabolism. Therefore, in the present study we

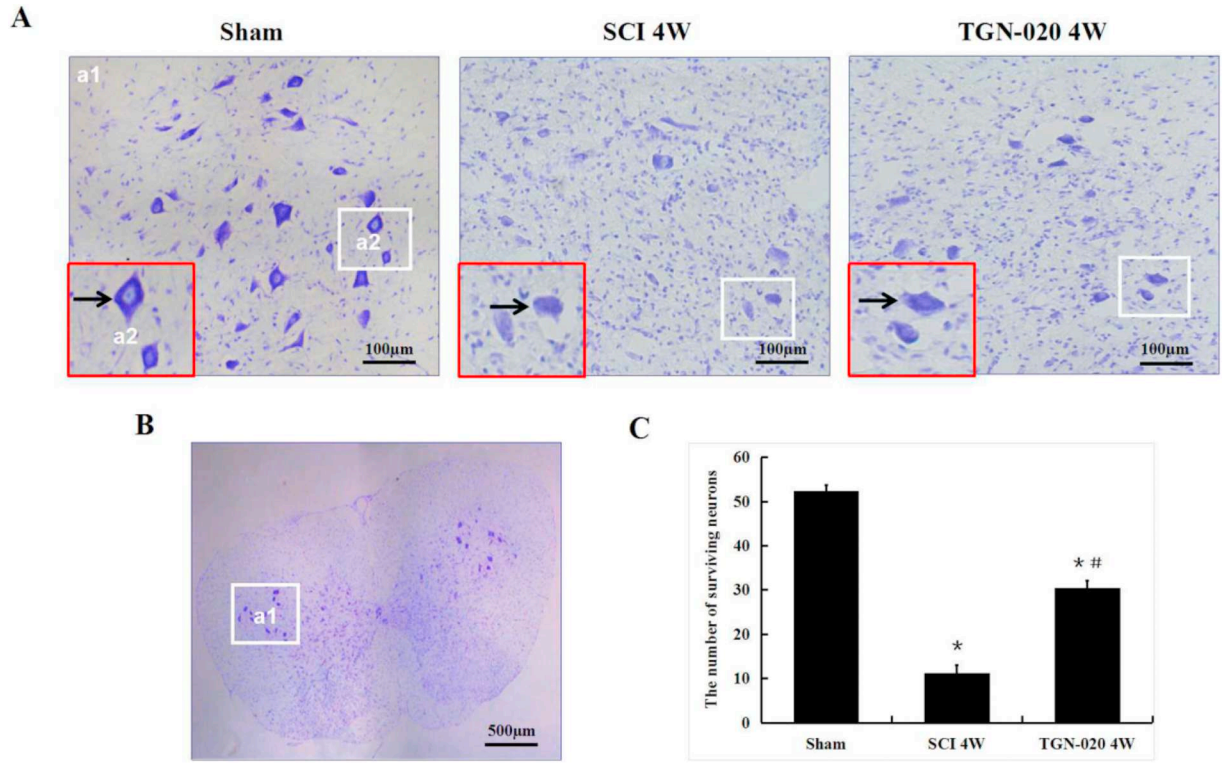

Fig. 6. Effects of TGN-020 on the surviving neurons at 4 weeks after SCI. (A) Nissl staining exhibited the number of surviving neurons at each group. (B) Nissl-positive neurons were mainly detected in the ventral horns of normal spinal cords. (C) Quantitative analysis of surviving neuronal number. Data are expressed as mean ± SEM, $p < 0.05$ was considered significant ($n = 5$, $^{*}p < 0.01$ versus the sham group; $^{\#}p < 0.01$ versus the SCI group. Scale bars: 100 μm or 500 μm).

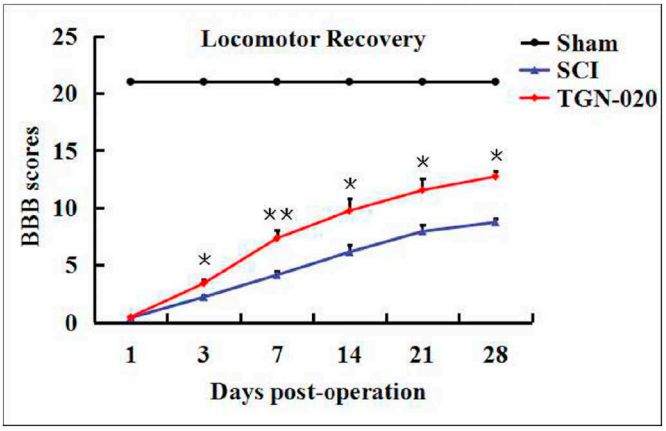

Fig. 7. Effects of TGN-020 on locomotor recovery at 1, 3, 7, 14, 21, and 28 days after SCI using BBB scores. As showed, sham group showed 21 scores at all time-points, compared with the SCI group, rats in the TGN-020 group showed the significantly higher scores from day 3 to day 28 after SCI. Data are expressed as mean ± SEM, $p < 0.05$ was considered significant ($n = 5$, $^{**}p < 0.01$ versus the SCI group for day 7; $^{*}p < 0.05$ versus the SCI group for days 3, 14, 21, and 28).

used 100 mg/kg TGN-020 administered intraperitoneally [30,31,43] to investigate changes in spinal cord edema and glial scar formation after SCI in rats. Certainly, our deficiency in this experiment is that we failed to afford the experiment results of dose-response to determine the optimal effective dosage of TGN-020 on SCI.

Secondary edema can result from increased intracellular or extracellular spinal cord water content [44], which can reportedly emerge within minutes of injury and peak 3 days thereafter [45]. AQP4 plays an important role in maintaining the homeostasis of water and ions in the CNS, and is involved in SCI-induced edema [5,46]. There is evidently a parallel correlation between AQP4 and spinal cord edema [34,47], and AQP4 expression is reportedly markedly rapidly upregulated at the acute phase, and maintains at high levels until 7 days, which is in conjunction with increased water content of tissues in spinal cord injury in rats [48]. Recent studies suggest that a single intraperitoneal injection of TGN-020 after an ischemic event can reduce brain edema and infarct volume in a rat model of cerebral ischemia [30,31]. In the present study, we examined the water content of tissues as an indication of the level of spinal cord edema 3 days after SCI. The results suggested that spinal cord water content was substantially increased at 3 days after SCI, which was significantly attenuated by the treatment with TGN-020. Both western blotting and immunofluorescence staining showed that AQP4 expression was substantially increased at day 3 after SCI, and TGN-020 administration could significantly decrease its expression. Collectively, these results suggested that TGN-020 could effectively reduce early spinal cord edema caused by SCI, via the inhibition of AQP4 expression.

Following SCI, astrocytes are activated and initially confer neuroprotective effects [16,17]. They subsequently become hypertrophic and proliferative, and migrate toward the injured site where they form a dense network of glial scarring, which acts as a physical and chemical barrier and has a negative effect on SCI recovery [18,19,49]. Suppression of glial scar formation is believed to provide a favorable environment for axonal regeneration and recovery of locomotor function after SCI [50–52]. The processes involved in astrocyte activation include specific molecular and morphological changes that are considered hallmarks of responses to CNS injuries [53]. GFAP is an intermediate filament protein, and increased GFAP expression indicates astrocyte proliferation and hypertrophy of the injured area [38]. Astrocyte activation is also evidenced by an increase in PCNA, which has been used as a general marker of dividing cells after SCI [39]. In some previous studies, astrocyte proliferation was markedly increased at day 3 after SCI [54]. Ge et al. [60], Zu et al. [35], and Liu et al. [59] have all reported that downregulation of AQP4 was accompanied by a reduction

in GFAP expression. It has also been reported that the AQP4 inhibitor TGN-020 significantly reduced gliosis after ischemic brain injury in vivo [30,43], and inhibited optic nerve astrocytes exposed to glutamate induced an increase in the expression of GFAP in vitro [27]. Our current data revealed that induction of spinal cord compression dramatically increased the expression levels of both GFAP and PCNA around the epicenters of the lesions at day 3 in rats, implying that astrocyte proliferation was markedly increased, and TGN-020 administration was observed to significantly combat the expression of GFAP and PCNA. Interestingly, our immunofluorescence double-staining results suggested that the coexpression of GFAP and PCNA was not totally coincident, which may be explained for the other cells proliferation, such as microglial or endothelial cells [55,56]. Our hematoxylin and eosin staining results revealed large and irregular cavities in injured spinal cords at 4 weeks. The cavities were significantly smaller in the TGN-020 group than they were in the SCI group. Collectively, the results showed that SCI induced substantial astrocyte proliferation near the center of the injury at day 3, and caused glial scar formation at 4 weeks, which is concordant with the results of a previous study [54]. TGN-020 administration effectively inhibited the activation of astrocytes after SCI, reducing glial scar formation.

The cytoplasmic and membrane-associated protein GAP-43 is highly enriched in neuronal growth cones, and its upregulation is considered to indicate the growth of axonal endings during development, and regeneration in the CNS [40]. In the current study, SCI induced GAP-43 expression around the lesion area, promoting neural regeneration at 4 weeks after spinal cord compression injury, which is concordant with the results of a previous study [57,58]. Interestingly, administration of TGN-020 significantly increased the levels of GAP-43, as well as neuron survival in the vicinity of the lesion at 4 weeks after SCI, in conjunction with remarkable functional improvement as determined by the BBB scale over the 4-week period. These data constitute the first reported indication that TGN-020 can promote axonal regeneration and increase neuron survival at 4 weeks after SCI in rats—which is useful with regard to facilitating functional recovery—and provide new insights into the treatment of SCI.

Previous studies have shown that numerous drugs including epigallocatechin-3-gallate, curcumin, and melatonin can inhibit SCI-induced AQP4 upregulation, and that these effects can reduce spinal cord edema and the expression of GFAP after SCI in rats [35,59,60]. Notably however, none of these agents specifically inhibit only AQP4 expression. In the present study, we found that TGN-020 administration significantly inhibited the expression of AQP4 and proteins associated with astrocyte proliferation, and reduced edema and glial scar formation after SCI. Furthermore, observations 4 weeks after SCI revealed that TGN-020 protected neural tissues and promoted axonal regeneration after severe damage. These results suggest that TGN-020 has therapeutic potential with regard to reducing secondary injury caused by SCI. However, this experiment benefits far more than the antocular conclusions. After various types of injuries, astrocyte activation is accompanied by significantly increased AQP4 throughout perivascular astrocytic endfeet [61,62]. In the current study, inhibition of astrocyte activation was associated with the downregulation of AQP4. This suggests that there may be a close relationship between edema and glial scar formation after SCI in rats, and AQP4 may be involved in the regulation of astrocyte proliferation and glial scar formation. Notably however, the intrinsic mechanisms involved remain unclear and further studies should be performed in the future.

Funding

This work was supported by the National Natural Science Foundation of China (grant numbers 81501659; 81471853); and the Science and Technology Planning Project of Liaoning Province (grant number 201602277).

Conflict of interest statement

The authors declare that there are no conflicts of interest.

Acknowledgements

The authors sincerely thank Prof. Zhongkai Fan (Jinzhou Medical University) and Ph.D. Gang Li (Tongji University) for assisting to design the experiments and revise the manuscript. We thank Jing Bi and Yang Cao for technical support. We also thank Wen Xu and Zhiqiang Jia for data analysis, and Mingchao Zhang and Weidong Guo for animal care. Finally, we thank the Key Laboratory of Neurodegenerative Diseases of Liaoning Province, Jinzhou Medical University.

References

[1] Yuan, J., Zou, M., Xiang, X., Zhu, H., Chu, W., & Liu, W., et al. (2015). Curcumin improves neural function after spinal cord injury by the joint inhibition of the intracellular and extracellular components of glial scar. J. Surg. Res., 195(1), 235.
[2] R.B. Borgens, P. Liu-Snyder, Understanding secondary injury, Q. Rev. Biol. 87 (2) (2012) 89–127.
[3] J.W. Mcdonald, C. Sadowsky, Spinal-cord injury, Lancet 359 (9304) (2002) 417–425.
[4] C.H. Tator, M.G. Fehlings, Review of the secondary injury theory of acute spinal cord trauma with emphasis on vascular mechanisms, J. Neurosurg. 75 (1) (1991) 15–26.
[5] N. Ning, X. Dang, C. Bai, C. Zhang, K. Wang, Panax notoginsenoside produces neuroprotective effects in rat model of acute spinal cord ischemia–reperfusion injury, J. Ethnopharmacol. 139 (2) (2012) 504–512.
[6] Y.B. Yang, Y.J. Piao, Effects of resveratrol on secondary damages after acute spinal cord injury in rats, Acta Pharmacol. Sin. 24 (7) (2003) 703.
[7] M.K. Oklinski, J.S. Lim, H.J. Choi, P. Oklinska, M.T. Skowronski, T.H. Kwon, Immunolocalization of water channel proteins AQP1 and AQP4 in rat spinal cord, J. Histochem. Cytochem. 62 (8) (2014) 598–611.
[8] D. Han, M. Sun, P.P. He, L.L. Wen, H. Zhang, J. Feng, Ischemic postconditioning alleviates brain edema after focal cerebral ischemia reperfusion in rats through down-regulation of aquaporin-4, J. Mol. Neurosci. 56 (3) (2015) 722–729.
[9] G.T. Manley, M. Fujimura, T. Ma, N. Noshita, F. Filiz, A.W. Bollen, et al., Aquaporin-4 deletion in mice reduces brain edema after acute water intoxication and ischemic stroke, Nat. Med. 6 (2) (2000) 159.
[10] O. Bloch, M.C. Papadopoulos, G.T. Manley, A.S. Verkman, Aquaporin-4 gene deletion in mice increases focal edema associated with staphylococcal brain abscess, J. Neurochem. 95 (1) (2010) 254–262.
[11] M.C. Papadopoulos, G.T. Manley, S. Krishna, A.S. Verkman, Aquaporin-4 facilitates reabsorption of excess fluid in vasogenic brain edema, FASEB J. 18 (11) (2004) 1291–1293.
[12] M.C. Papadopoulos, A.S. Verkman, Aquaporin-4 and brain edema, Pediatr. Nephrol. 22 (6) (2007) 778–784.
[13] S. Saadoun, B.A. Bell, A.S. Verkman, M.C. Papadopoulos, Greatly improved neurological outcome after spinal cord compression injury in AQP4-deficient mice, Brain 131 (Pt 4) (2008) 1087–1098.
[14] S. Karimiabdolrezaee, R. Billakanti, Reactive astrogliosis after spinal cord injury—beneficial and detrimental effects, Mol. Neurobiol. 46 (2) (2012) 251–264.
[15] N. Medicine, Conditional ablation of STAT3 or SOCS3 discloses a dual role for reactive astrocytes after spinal cord injury, Nat. Med. 12 (7) (2006) 829–834.
[16] L. Li, A. Lundkvist, D. Andersson, U. Wilhelmsson, N. Nagai, A.C. Pardo, et al., Protective role of reactive astrocytes in brain ischemia, J. Cereb. Blood Flow Metab. 28 (3) (2008) 468–481.
[17] S. Saadoun, M.C. Papadopoulos, H. Watanabe, D. Yan, G.T. Manley, A.S. Verkman, Involvement of aquaporin-4 in astroglial cell migration and glial scar formation, J. Cell Sci. 118 (24) (2005) 5691–5698.
[18] B. Lin, X.U. Yang, B.I. Zhang, H.E. Yong, Y. Yan, H.E. Mingchang, MEK inhibition reduces glial scar formation and promotes the recovery of sensorimotor function in rats following spinal cord injury, Exp. Ther. Med. 7 (1) (2014) 66–72.
[19] J. Silver, J.H. Miller, Regeneration beyond the glial scar. Nat Rev Neurosci 5:146–156, Nat. Rev. Neurosci. 5 (2) (2004) 146–156.
[20] K.I. Auguste, S. Jin, K. Uchida, D. Yan, G.T. Manley, M.C. Papadopoulos, et al., Greatly impaired migration of implanted aquaporin-4-deficient astroglial cells in mouse brain toward a site of injury, FASEB J. 21 (1) (2007) 108.
[21] D.C. Lu, Z. Zador, J. Yao, F. Fazlollahi, G.T. Manley, Aquaporin-4 reduces post-traumatic seizure susceptibility by promoting astrocytic glial scar formation in mice, J. Neurotrauma (2011).
[22] M.V. Sofroniew, Reactive astrocytes in neural repair and protection, Neuroscientist 11 (5) (2005) 400.
[23] Fan, Y., Kong, H., Shi, X., Sun, X., Ding, J., & Wu, J., et al. (2008). Hypersensitivity of aquaporin 4-deficient mice to 1-methyl-4-phenyl-1,2,3,6-tetrahydropyrindine and astrocytic modulation. Neurobiol. Aging, 29(8), 1226–1236.
[24] Huang, X., Kim, J. M., Kong, T. H., Park, S. R., Ha, Y., & Kim, M. H., et al. (2009). GM-CSF inhibits glial scar formation and shows long-term protective effect after spinal cord injury. J. Neurol. Sci., 277(1–2), 87–97.
[25] H. Igarashi, V.J. Huber, M. Tsujita, T. Nakada, Pretreatment with a novel aquaporin

4 inhibitor, TGN-020, significantly reduces ischemic cerebral edema, Neurol. Sci. 32 (1) (2011) 113–116.
[26] Y. Nakamura, Y. Suzuki, M. Tsujita, V.J. Huber, K. Yamada, T. Nakada, Development of a novel ligand, [11c]TGN-020, for aquaporin 4 positron emission tomography imaging, ACS Chem. Neurosci. 2 (10) (2011) 568.
[27] Nishikawa, Y., Oku, H., Morishita, S., Horie, T., Kida, T., & Mimura, M., et al. (2016). Negative impact of AQP-4 channel inhibition on survival of retinal ganglion cells and glutamate metabolism after crushing optic nerve. Exp. Eye Res., 146, 118.
[28] Wei, F., Zhang, C., Xue, R., Shan, L., Gong, S., & Wang, G., et al. (2017). The pathway of subarachnoid CSF moving into the spinal parenchyma and the role of astrocytic aquaporin-4 in this process. Life Sci., 182, 29–40.
[29] H. Igarashi, M. Tsujita, Y. Suzuki, I.L. Kwee, T. Nakada, Inhibition of aquaporin-4 significantly increases regional cerebral blood flow, Neuroreport 24 (6) (2013) 324–328.
[30] I. Pirici, T.A. Balsanu, C. Bogdan, C. Margaritescu, T. Divan, V. Vitalie, et al., Inhibition of aquaporin-4 improves the outcome of ischaemic stroke and modulates brain paravascular drainage pathways, Int. J. Mol. Sci. 19 (1) (2018) 46.
[31] Popescu, E. S., Pirici, I., Ciurea, R. N., Bălşeanu, T. A., Cătălin, B., & Mărgăritescu, C., et al. (2017). Three-dimensional organ scanning reveals brain edema reduction in a rat model of stroke treated with an aquaporin 4 inhibitor. Romanian J. Morphol. Embryol., 58(1), 59.
[32] Leitã£O, R. A., Sereno, J., Castelhano, J. M., Gonã§Alves, S. I., Coelho-Santos, V., & Fontes-Ribeiro, C., et al. (2018). Aquaporin-4 as a new target against methamphetamine-induced brain alterations: focus on the neurogliovascular unit and motivational behavior. Mol. Neurobiol., 55(3), 2056–2069.
[33] Ropper, A. E., Zeng, X., Anderson, J. E., Yu, D., Han, I., & Haragopal, H., et al. (2015). An efficient device to experimentally model compression injury of mammalian spinal cord. Exp. Neurol., 271, 515–523.
[34] Fan, Z. K., Wang, Y. F., Cao, Y., Zhang, M. C., Zhang, Z., & Lv, G., et al. (2010). The effect of aminoguanidine on compression spinal cord injury in rats. Brain Res., 1342(1), 1–10.
[35] J. Zu, Y. Wang, G. Xu, J. Zhuang, H. Gong, J. Yan, Curcumin improves the recovery of motor function and reduces spinal cord edema in a rat acute spinal cord injury model by inhibiting the JAK/STAT signaling pathway, Acta Histochem. 116 (8) (2014) 1331–1336.
[36] D.S. Tian, Y.U. Zhi-Yuan, M.J. Xie, B.U. Bi-Tao, O.W. Witte, W. Wang, Suppression of astroglial scar formation and enhanced axonal regeneration associated with functional recovery in a spinal cord injury rat model by the cell cycle inhibitor olomoucine, J. Neurosci. Res. 84 (2) (2006) 74–83.
[37] D.M. Basso, M.S. Beattie, J.C. Bresnahan, A sensitive and reliable locomotor rating scale for open field testing in rats, J. Neurotrauma 12 (1) (1995) 1.
[38] M. Pekny, M. Pekna, Astrocyte intermediate filaments in CNS pathologies and regeneration, J. Pathol. 204 (4) (2004) 428–437.
[39] Huang, S., Liu, X., Zhang, J., Bao, G., Xu, G., & Sun, Y., et al. (2015). Expression of peroxiredoxin 1 after traumatic spinal cord injury in rats. Cell. Mol. Neurobiol., 35(8), 1217–1226.
[40] Aigner, L., Arber, S., Kapfhammer, J. P., Laux, T., Schneider, C., & Botteri, F., et al. (1995). Overexpression of the neural growth-associated protein GAP-43 induces nerve sprouting in the adult nervous system of transgenic mice. Cell, 83(2), 269–78.
[41] S.M. Onifer, A.G. Rabchevsky, S.W. Scheff, Rat models of traumatic spinal cord injury to assess motor recovery, ILAR J. 48 (4) (2007) 385.
[42] Zhao, L., Li, D., Liu, N., Liu, L., Zhang, Z., & Gao, C., et al. (2018). Correlation of TGN-020 with the analgesic effects via ERK pathway activation after chronic constriction injury. Mol. Pain, 14.
[43] Catalin, B., Pirici, I., Balseanu, T. A., Stan, A., Tudorica, V., & Balea, M., et al. (2018). Cerebrolysin and aquaporin 4 inhibition improve pathological and motor recovery after ischemic stroke. CNS Neurol. Disord. Drug Targets, 17(4).
[44] Nesic, O., Lee, J., Ye, Z., Unabia, G. C., Rafati, D., & Hulsebosch, C. E., et al. (2006). Acute and chronic changes in aquaporin 4 expression after spinal cord injury. Neuroscience, 143(3), 779–792.
[45] M. Lemke, A.I. Faden, Edema development and ion changes in rat spinal cord after impact trauma: injury dose-response studies, J. Neurotrauma 7 (1) (1990) 41–54.
[46] S. Saadoun, M.C. Papadopoulos, Aquaporin-4 in brain and spinal cord oedema, Neuroscience 168 (4) (2010) 1036–1046.
[47] K. Oshio, D.K. Binder, B. Yang, S. Schecter, A.S. Verkman, G.T. Manley, Expression of aquaporin water channels in mouse spinal cord, Neuroscience 127 (3) (2004) 685–693.
[48] Y. Xiaodong, L. Juanfang, W. Xiji, L. Wenhao, C. Jingyuan, S. Honghui, Pretreatment with AQP4 and NKCC1 inhibitors concurrently attenuated spinal cord edema and tissue damage after spinal cord injury in rats, Front. Physiol. 9 (2018) (6-).
[49] Y.M. Yuan, C. He, The glial scar in spinal cord injury and repair, Neurosci. Bull. 29 (4) (2013) 421–435.
[50] V.J. Huber, M. Tsujita, T. Nakada, Identification of aquaporin 4 inhibitors using in vitro and in silico methods, Bioorg. Med. Chem. 17 (1) (2009) 411–417.
[51] Liu, Y., Ban, D. X., Ma, C., Zhang, Z. G., Zhang, J. Y., & Gao, S. J., et al. (2016). Photodynamic therapy mediated by upconversion nanoparticles to reduce glial scar formation and promote hindlimb functional recovery after spinal cord injury in rats. J. Biomed. Nanotechnol., 12(11), 2063–2075.
[52] Okuda, A., Horiihayashi, N., Sasagawa, T., Shimizu, T., Shigematsu, H., & Iwata, E., et al. (2016). Bone marrow stromal cell sheets may promote axonal regeneration and functional recovery with suppression of glial scar formation after spinal cord transection injury in rats. J. Neurosurg. Spine, 26(3), 1.
[53] B. Pathology, GFAP and astrogliosis, Brain Pathol. 4 (3) (1994) 229–237.
[54] Li, G., Cao, Y., Shen, F., Wang, Y., Bai, L., & Guo, W., et al. (2016). Mdivi-1 inhibits astrocyte activation and astroglial scar formation and enhances axonal regeneration after spinal cord injury in rats. Front. Cell. Neurosci., 10.
[55] J.M. Krum, A. Khaibullina, Inhibition of endogenous VEGF impedes revascularization and astroglial proliferation: roles for vegf in brain repair, Exp. Neurol. 181 (2) (2003) 241–257.
[56] Tian, D. S., Xie, M. J., Yu, Z. Y., Zhang, Q., Wang, Y. H., & Chen, B., et al. (2007). Cell cycle inhibition attenuates microglia induced inflammatory response and alleviates neuronal cell death after spinal cord injury in rats. Brain Res., 1135(1), 177–185.
[57] R. Curtis, D. Green, R.M. Lindsay, G.P. Wilkin, Up-regulation of GAP-43 and growth of axons in rat spinal cord after compression injury, J. Neurocytol. 22 (1) (1993) 51–64.
[58] G.L. Li, M. Farooque, A. Holtz, Y. Olsson, Increased expression of growth-associated protein 43 immunoreactivity in axons following compression trauma to rat spinal cord, Acta Neuropathol. 92 (1) (1996) 19.
[59] Liu, X., Wang, Y., Yang, J., Liu, Y., Zhou, D., & Hou, M., et al. (2015). Anti-edema effect of melatonin on spinal cord injury in rats. Biomed. Pap. Med. Fac. Univ. Palacky Olomouc Czech Repub., 159(2), 220–226.
[60] R. Ge, Y. Zhu, Y. Diao, L. Tao, W. Yuan, X.C. Xiong, Anti-edema effect of epigallocatechin gallate on spinal cord injury in rats, Brain Res. 1527 (35) (2013) 40–46.
[61] P.K. Eide, V.A. Eidsvaag, E.A. Nagelhus, H.A. Hansson, Cortical astrogliosis and increased perivascular aquaporin-4 in idiopathic intracranial hypertension, Brain Res. 1644 (2016) 161–175.
[62] Sun, L., Li, M., Ma, X., Zhang, L., Song, J., & Lv, C., et al. (2018). Inhibiting high mobility group box-1 reduces early spinal cord edema and attenuates astrocyte activation and aquaporin-4 expression after spinal cord injury in rats. J. Neurotrauma.